Bernhard K. J. Viertel*, Ady Naber, Simon Hoffmann, Daniel Berwanger, Lucy Kessler, Ramin Khoramnia and Werner Nahm

# Automated vessel centerline extraction and diameter measurement in OCT Angiography

**Abstract:** Optical Coherence Tomography Angiography (OCTA) is a non-invasive imaging technique that enables the visualization of perfused vasculature in vivo. In ophthalmology, it allows the physician to monitor diseases affecting the vascular networks of the retina such as age-related macular degeneration or diabetic retinopathy. Due to the complexity of the vasculature in the retina, it is of interest to automatically extract vascular parameters which describe the condition of the vessels. Suitable parameters could improve the diagnosis and the treatment during the course of therapy. We present an automated algorithm to compute the diameters of the vessels in en face OCTA images. After segmenting the images, the vessel centerline was computed using a thinning algorithm. The centerline was refined by detecting invalid pixels such as spurs and by continuing the centerline until the ends of the vessels. Lastly, the diameter was computed by dilating a discrete circle at the position of the centerline or by measuring the distance between both borders of the vessels. The developed algorithms were applied to in vivo images of human eyes. Certainly, no ground truth was available. Hence, a plausibility check was performed by comparing the measured diameters of two different layers of the retina (Superficial Vascular Complex (SVC) and Deep Vascular Complex (DVC)). Each layer exhibits a different characteristic vasculature. The algorithm clearly reflected the differences from both retinal layers. The measured diameters demonstrate that the DVC consists of more capillaries and considerably smaller vessels compared to the SVC. The presented method enables automated analysis of the retinal vasculature and forms thereby the basis for monitoring diseases influencing the vasculature of the retina. The validation of the method using an artificial ground truth is still needed.

---

**\*Corresponding author: Bernhard K. J. Viertel:** Institute of Biomedical Engineering, Karlsruhe Institute of Technology, Kaiserstraße 12, Karlsruhe, Germany, e-mail: publications@ibt.kit.edu
**Ady Naber, Simon Hoffmann, Daniel Berwanger and Werner Nahm:** Institute of Biomedical Engineering, Karlsruhe Institute of Technology, Kaiserstraße 12, Karlsruhe, Germany
**Lucy Kessler and Ramin Khoramnia:** Department of Ophthalmology, Heidelberg Klinikum, Heidelberg, Germany

## 1 Introduction

Common diseases such as age-related macular degeneration (AMD) or diabetic retinopathy (DR) can cause retinal neovascularization that can heavily impair the visual acuity. The neovascularization can be reduced by performing a treatment with Anti-VEGF agents [1]. The monitoring of the treatment can be conducted in vivo using Optical Coherence Tomography Angiography (OCTA) [1]. In contrast to fluorescein angiography, OCTA is a non-invasive imaging technique that enables three-dimensional visualization of the blood vessels in the retina. Due to the complexity of the retinal vasculature and the high resolution of the OCTA images, it is of interest to automatically extract geometrical and morphological parameters of the vessels to quantify the degree of neovascularization. Some key vascular parameters are the vessel area density, vessel length density, vessel tortuosity, vessel branching angle and vessel diameter [2][3]. The vessel diameter, in particular, could be a promising metric to quantify and assess neovascularization since it extracts detailed morphological characteristics about each individual vessel and enables the examination of vessels with a certain caliber. In 2016, Chu et al. introduced the vessel diameter index (VDI) that calculates the average diameter within a certain window section of the image [2]. A superior method was presented by Wei et al. that calculates the diameter of each individual vessel based on the binarized vessels and the vessel skeleton [3]. The skeleton was calculated using a thinning algorithm. Based on the gradient of the skeleton, searching directions were defined to compute the minimum radial distances from the skeleton to its nearest vessel boundary. The method yielded good results except for 90 degree corners. Similar to Wei's approach, our presented diameter measurement utilizes the segmented en face OCTA image and the vessel centerline. The vessel centerline or skeleton in OCTA images is often computed using thinning algorithms [2][3]. These algorithms create two issues in the resulting centerline that are often neglected. Firstly, the centerline does not cover the whole vessels because

in most cases the ends of the vessels are not reached. Secondly, due to irregular boundaries the formation of spurs is possible. Spurs are additional junctions that contain invalid pixels because they do not represent the actual course of the centerline. Those two issues are addressed in the presented methods. Finally, the diameter of each individual vessel is computed by dilating a discrete circle until it reaches the boundary of the vessels or by measuring the distance between both borders of the vessels. The developed algorithms were applied to in vivo en face OCTA images of human eyes. Since no ground truth was available, a plausibility check was performed to answer the question whether the presented method reflects the basic vascular differences between two distinct layers of the retina. Specifically, the measured diameters of the Superficial Vascular Complex (SVC) and the Deep Vascular Complex (DVC) were compared. The DVC contains capillaries in contrast to the SVC which consists of arterioles, venules and capillaries [4].

# 2 Material and Methods

55 eyes were imaged at the Universitätsklinikum Heidelberg with the Spectralis OCTA (Spectralis, Heidelberg Engineering, Heidelberg, Germany). The images were centered at the fovea. A 10°x10° (~2.9 x ~2.9 mm) scan pattern with a lateral resolution of 5.7 μm/pixel and an axial resolution of 3.9 μm/pixel (512 A-Scans x 512 B-Scans) was used. For each eye the corresponding en face OCTA images of the DVC and SVC were extracted (see figure 1).

## 2.1 Image segmentation

The segmentation of the en face OCTA images is not in focus of the study and generally an arbitrary method can be used. In short, the Optimally Oriented Flux (OOF) was first applied to detect and enhance vessels [5]. Afterwards, connected structures were identified by an initial binarization using Otsu's method with a sliding window. The average grey value of a connected structure was added to its pixels to improve the contrast of the image. After the enhancement of the vessels, two separate regions were visible in the image histogram so that the final segmentation into vessels and background tissue could be performed with Otsu's method.

## 2.2 Centerline extraction

After binarizing the image, the initial centerline was computed using a thinning algorithm [6]. To detect invalid pixels such as

spurs and to correct the lack of pixels at the ends of the vessels, the direction of the vessel was utilized. Additional to the spurs, pixels of the centerline that connected two vessels were considered invalid because they didn't satisfy the condition for the diameter measurement and wouldn't occur if the vessels would be separate. The direction of the vessel can be extracted using the corresponding eigenvector of the absolute smallest eigenvalue (the eigenvalue closest to zero) of the OOF for each pixel of the centerline if the pixel is inside the binary mask and the local circle touches the boundary of the vessel. Thus, the computation of the direction depends strongly on the radius, the diameter measurement (chapter 2.3) was used to determine the appropriate radius of the pixel under investigation. The direction of the vessel was used to continue the centerline until the ends of the vessel. The influence of faulty directions was reduced by adding only new pixels if no centerline was located orthogonally from the vessel direction at the position of the new pixels. A common method for the detection of spurs is to compare the spur length and the length of the main vessel. However, the length is not a valid metric for the complex course of the vessels in en face OCTA images that have lots of branches with vessels of different sizes. Nevertheless, the detection of invalid pixels of the centerline could be performed by comparing the direction of the vessel with the direction of the centerline. This is based on the assumption that a centerline is a representation of its corresponding structure and thereby the direction of the centerline and the vessel should be similar. The direction of the centerline was defined with 3x3 pixel masks and corresponding directions. If the mask corresponded to the 8-neighbourhood of the pixel under investigation, the respective direction was assigned to the pixel. For pixels such as branch pixels that had no clear centerline direction based on the 8-neighbourhood no direction could be assigned. Both directions were compared for each feasible pixel of the centerline and pixels with an angular difference greater than the threshold of 45 degrees were considered invalid. The angular difference was defined as the minimum angle between the lines along both directions. Potential spurs were defined between endpoints and branchpoints. A potential spur with more than two pixels was completely removed and considered a spur if it had at least as many invalid pixels as valid pixels without taking the additional pixels at the ends into consideration. The final step was the exclusion of the remaining invalid pixels that were not end pixels and the elimination of redundant pixels of the centerline.

## 2.3 Diameter measurement

The diameters of the vessels were computed for each pixel of the centerline. The main measurement was based on the

dilation of a discrete circle with radius $r_d \in \mathbb{N}$ centered at the pixel under investigation until the circle with radius $r_{d,max}$ was just larger than the segmented vessel area so that the circle overlapped with the background tissue. This method depends on the condition that the pixel under investigation is located in the middle of the binary structure with a sufficient distance to the end of the structure. Therefore, the dilation of the discrete circle is not appropriate for the additional pixels at the ends of the vessel. Instead, the method is applied to each pixel of the initial centerline after the thinning. Generally, the diameters of discrete circles are defined as $2 * r_d + 1$ so that the diameters can only obtain uneven numbers. Hence, for a correct diameter measurement a differentiation between even $2 * r_{d,max}$ and uneven $2 * (r_{d,max} - 1) + 1$ diameters had to be performed. The distinction was executed by checking whether the last circle with the diameter $2 * r_{d,max} + 1$ overlapped only on one side or on two opposite sides. The first case indicated an even and the second case an uneven diameter. A heuristic was defined that investigates the centroid of the overlapping pixels and divides the maximum size circle into an inner circle with radius $1/\sqrt{2} * r_{d,max}$ and an outer part that has the same area. If the overlapping pixels were symmetrically distributed, the centroid was within the inner circle and the uneven diameter was assigned to the pixel under investigation. Otherwise, a second examination was conducted by moving the circle with the maximum size by one pixel towards a certain direction. The direction was defined from the centroid to the midpoint of the circle. If the centroid of the second examination was once again outside the inner circle the even diameter was assigned to the pixel under investigation. If the centroid was within the inner circle the uneven diameter was used. Another case could be that the circle is completely inside the vessel with no overlapping pixels. This indicates that the pixel under investigation is not in the middle of the binary structure. Still, the diameter $2 * r_{d,max} + 1$ was assigned to the pixel. The operating principles of this approach were validated and yielded good results. The second diameter measurement involved the computation of the absolute distance between both borders of the segmented vessels based on the orthogonal axes of the direction of the vessel. The direction was extracted using the OOF (see chapter 2.2). Due to the measurement along a direction the method could be applied to all additional pixels of the centerline at the ends of the vessels.

# 3 Results

Due to low image quality 46 eyes had to be exclude so that 9 eyes were used for the comparison of the vessel diameters in the DVC and SVC. The resolution of the images was by virtue

of the scales per image between 3.23 μm/pixel and 3.57 μm/pixel. Example en face OCTA images of the DVC and SVC from the same eye are visualized in figure 1. It is visible that the SVC consists of larger vessels compared to the DVC.
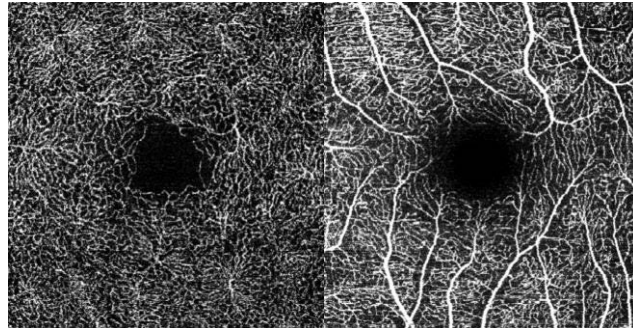


**Figure 1:** En face OCTA image of the DVC (left) and of the SVC (right) from the same eye.
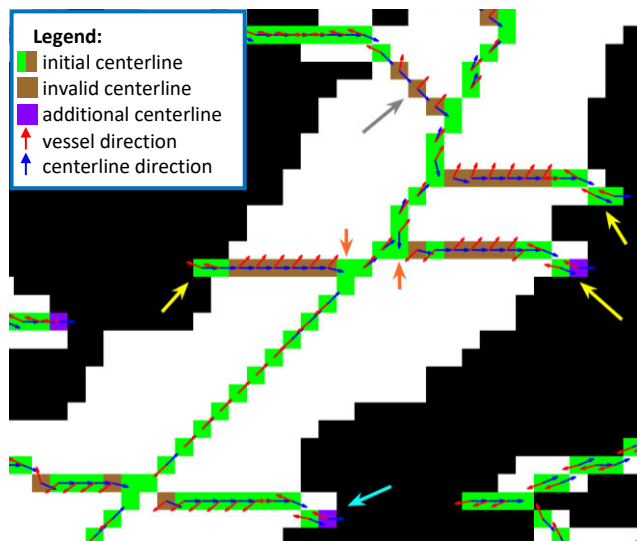


**Figure 2:** Exemplary image section of a segmented en face OCTA image that depicts the application of the centerline correction methods. The yellow arrows point at spurs that are completely removed, in contrast to the cyan colored arrow that points at a spur that should have been removed. The orange arrows mark redundant pixels and the as invalid detected pixels that connect to vessel branches are marked with the gray arrow.

An exemplary illustration of the methods for the correction of the centerline is shown in figure 2. The diameters of the vessels in the en face OCTA images were combined for each individual image into a diameter histogram with a bin size of one pixel. The percentage differences of the number of measured diameters per diameter category between the SVC and DVC of the same eyes were computed. The percentage differences for the 9 eyes were combined for each category into boxplots that are depicted in figure 3. The maximum measured vessel diameters in the SVC and DVC of the individual eyes were between 15 and 27 pixels so that the maximum bin of figure 3 was set to 15.
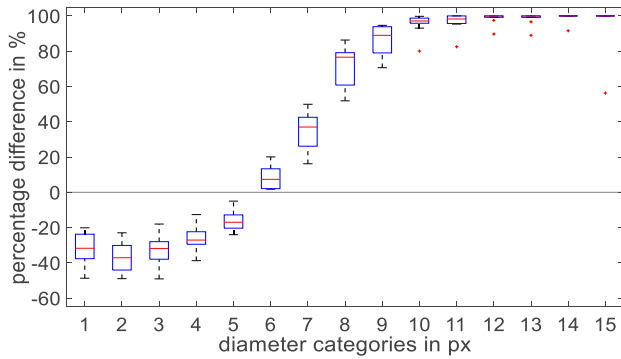
**Figure 3:** Percentage differences of the number of measured diameters between the SVC and DVC per diameter category for all 9 eyes. The bin size is one and symmetrically distributed around the diameter category. A negative percentage difference represents that the DVC consisted of more measured diameters compared to the SVC and vice versa.

# 4 Discussion

In this study, methods were presented that improve the extraction of the vessel centerline by detecting invalid pixels such as spurs and by continuing the centerline until the ends of the vessels. Furthermore, a vessel diameter measurement that extracts detailed morphological vessel characteristics in en face OCTA images was introduced. The performance of the extraction of the centerline could not be quantitatively validated due to the application to in vivo images without having a ground truth. Though, an exemplary application is illustrated in figure 2. It is visible that an increased angular difference for invalid pixels such as spur pixels exist. Due to minor angular difference of spur pixels near the vessel boundary and because of a too large angular threshold for the definition of invalid pixels, it was not possible to identify every spur (see figure 2 cyan coloured arrow). Generally, the spur detection performs best for spurs that run orthogonally from the direction of the vessels and have few pixels near the boundary of the vessel compared to the length of the spur. In the future, a validation of the method in silico or with hand labelled data can be conducted to evaluate the performance and adjust the optimal angular threshold [7]. The continuing of the centerline until the ends of the vessels performed qualitatively well but should be validated with the methods described above. A major limitation of the study is that the diameter measurement in the context of the en face OCTA images could not be validated. Nevertheless, based on figure 3 it can be deduced that the DVC consists of more capillaries and considerably smaller vessels compared to the SVC. This confirms that the method can reflect the basic vascular differences between the two layers. The approach of Wei's

diameter measurement and our method is similar because both compute the minimal distances of the centerline towards the vessel boundary. However, the realization of our diameter measurement is different because Wei computes the minimal radial distance instead of a dilation of a discrete circle. Due to the discretization, the dilation of a discrete circle has the disadvantage to be less exact with narrower structures that run at an angle of about 45 degrees. This is the case, because discrete circles with a small radius have a poor proportion between the horizontal axes and the axes at 45 degrees. This issue could be improved by upsampling the image. The advantage of the dilation of a discrete circle is that it checks the diameter in every direction instead of defining a searching direction based on a gradient. The proposed algorithms are adaptable and can be applied to other image modalities. Further research should consider the validation of the methods with an artificial ground truth and the application within clinical context by assessing retinal neovascularization.

# References

[1] Marques JP, et al. Sequential Morphological Changes in the CNV Net after Intravitreal Anti-VEGF Evaluated with OCT Angiography. Ophthalmic Res 2016;55:145–151

[2] Chu Z, et al. Quantitative assessment of the retinal microvasculature using optical coherence tomography angiography. J. Biomed. Opt. 2016;21(6),066008

[3] Wei W, et al. Automated vessel diameter quantification and vessel tracing for OCT angiography. J. Biophotonics 2020; 13:e202000248

[4] Tan PEZ et al. Quantitative confocal Imaging of the Retinal Microvasculature in the Human Retina. iovs 2012;53:5728-5736

[5] Law MWK, Chung ACS. Three Dimensional Curvilinear Structure Detection Using Optimally Oriented Flux. ECCV 2008; LNCS 5305 pp.368-382

[6] Lam L, et al. Thinning Methodologies–A Comprehensive survey. IEEE Trans. Pattern Anal. Mach. a. Intell. 1992;14(9) p.879, bottom of first column trough top of second column

[7] Ma Y, et al. ROSE: A Retinal OCT-Angiography Vessel Segmentation Dataset and New Model. IEEE Transaction on Medical Imaging 2021;40(3):928-939